Characterization of scatter factors in thyroid studies using a pinhole collimator by Monte Carlo Simulation.

S. Rodríguez[1], A. López[2], A. Díaz[1], A. Palau[2], and JM. Martín[2]

[1] Department of Physics, Center of Applied Technology and Nuclear Development, Havana, Cuba
[2] Department of Nuclear Medicine, "Hermanos Ameijeiras" Hospital, Havana, Cuba

Abstract— **To study the scatter factors during I-131 thyroid scintigraphic studies with a pinhole collimator (5mm hole) was developed a Monte Carlo (MC) simulation using GAMOS code. First, to check the accuracy of the Monte Carlo model, simulated and measured data using a thyroid phantom were compared. The accuracy of the Monte Carlo model was verified by the good agreement between measured and simulated energy spectra and the maximum discrepancies of 2% in the counts/sec/MBq. Next, simulations to investigate scatter were performed for different tissue thickness between the thyroid and collimator (5-15mm). The image's scatter contribution was significant in the 5mm pinhole, being between 27-40%. On the basis of the separated scatter from direct count included in window energy spectra, a preliminary evaluation of multiple window energy correction methods was performed. For the simulated thyroid geometry with pinhole, the reduce inferior double energy window methods (15% on 364keV photopeak window) provides a reasonable correction for scatter. This study is the first approach; we recommend including real thyroid geometry with different thyroid depth-thickness and mass.**

Keywords— **Monte Carlo, GAMOS, thyroid studies, pinhole collimator, scatter.**

I. Introduction

Hyperthyroidism is a common disorder, with an estimated incidence varying from 25 cases per 100 000 persons per year in areas with high iodine intake to 38.7 per 100 000 in iodine deficient areas [1]. Radioiodine treatment of hyperthyroidism has been used since 1942, but after more than half a century and the treatment of hundreds of thousands of patients the question of the "optimal" radioiodine activity to administer still lacks a definitive answer [2,3,4]. Major changes in clinical practice should guide us to find and accurate dosimetry, capable to diminish the risks of adverse effects and the optimization of the treatment.

Until now, the dose dependent effects have not been analyzed in detail, in the majority of patient-specific treatment activity's calculation is derived from repeated probe measurements after administration of small doses of ^{131}I. While this procedure provides "accurate" data on uptake and effective half-life, it does not allow the evaluation of regional iodine metabolism or distribution. Internal radionuclide radiation dosimetry deals with the determination of the amount of spatial and temporal distribution of radiation energy deposited in tissue by radionuclides within the body [5]. It means using nuclear medicine images techniques and probe measurements for obtain all the information needed to specific-patient dose/activities estimation, treatment's planning and verification [6,7].

The pinhole generates magnified images of small organs like the thyroid, with high resolution and acceptable sensitivity. In ^{131}I images, quality and quantification accuracy are degraded by scatter and attenuation, and pinhole collimators are not the exception [8].

Monte Carlo method has the ability to simulate different independent physical processes. Because of this has been applied in medical physics to a wide range of problems that are difficult to study via analytical or experimental approaches [9,10].

Currently, there is a group of software packages whose structure has been programmed on the basis of general purpose codes such as MCNP and GEANT4. GATE, Penelope and GAMOS are known as specific purpose GEANT4 codes and they allow a dynamic and easy implementation of Gamma Cameras, SPECT and PET systems and their fundamental characteristics [11].

Present work was done using GAMOS package (GEANT-4 based Architecture for Medicine-Oriented Simulations). It facilitates the use of GEANT4 (GEometry ANd Tracking) by avoiding the need to use C++, providing, instead, a set of user commands. One of the novelties of GAMOS lies in its big flexibility, which make it appropriate for the simulation in many physics fields. This flexibility is supported by wide range of geometries, primary generators and physics lists as well as by set of tools that help the user in extracting detailed information through user commands. Besides, the so call "plug-in" technology contributes to its flexibility, as it facilitates to include extra functionality not foreseen by the framework authors [12].

The effects of penetration, object scatter and collimator scatter in quantitative pinhole studies depend not only on the energy of the photons emitted by the radionuclide; but also on the spatial distribution of the radioactive source. Previous work assessing scatter and penetration in ^{131}I imaging in pinhole collimator is limited to a few studies in

D.A. Jaffray (ed.), *World Congress on Medical Physics and Biomedical Engineering, June 7-12, 2015, Toronto, Canada*,
IFMBE Proceedings 51, DOI: 10.1007/978-3-319-19387-8_44

general dedicated to compensated resolution /scatter with Point /linear spread function in tumor geometry [13-17]. This research is focused on the improvement and optimization of thyroid-specific patient studies. Therefore its main goal is to demonstrate the feasibility of the use of Monte Carlo mathematical modeling for evaluation of the required thyroid studies, such as scatter, using gamma cameras in genuine medical environments. The characterization of energy and spatial distributions of scatter performed in this study by Monte Carlo simulation will be useful for the development and evaluation of techniques that compensate for such events in ^{131}I imaging.

II. Materials and Methods

The system to be model was the Philips Forte Gamma Camera of the Nuclear Medicine Department, in "Hermanos Ameijeiras" Hospital, with the pinhole collimator - 5 mm aperture cone for thyroid studies (Figure 1), which allows static and tomographic images of radiopharmaceuticals biodistribution.

Fig. 1 Philips Forte Gamma Camera with pinhole collimator, neck- thyroid's phantom used to MC simulation and verification, [1]Spine, [2]Trachea, [3]Thyroid

The collimator has a chamber covered by a lead shield on the rear side, which prevents the entry of photons originating outside the examined object. Detection system comprises a gantry with two NaI(Tl) scintillation crystals detectors mounted on a rotating basis. Each detector has 55 photomultiplier tubes, stimulated only if they are related to the specific radiation impact area on the crystal. Each detector has a field of view (FoV) of 38.1 cm × 50.8 cm and a thickness of 9.5 mm.

The image is magnified and inverted respect to the object. This configuration, fixed a 60º acceptance angle for the gamma rays, has a 25.4 mm septal thickness, a 22 cm focus-detector distance and a (FoV) of 25.4 cm. Estimations were performed using manufacturer-provided collimator parameters.

A. Model simulated by GAMOS

A geometric model identical to the experimental setup, phantom and the detection system, was developed using GAMOS text active commands. The most significant ^{131}I γ-ray emissions are at 364 keV (82%), 637 keV (7.2%), and 723 keV(1.8%), and typically imaging is carried out with a photopeak window at 364 keV. Input parameters were selected according to those used in the experimental measurements in order to verify its correspondence with the simulation data. In each thyroid lobe 50μCi activity source was defined. An isotropic spatial distribution was set for ^{131}I isotope source, which emits at 364 keV. Figure 2 shows the phantom geometry and gamma camera with pinhole collimator simulated by GAMOS and visualized using 3D "DeepViewer"software.

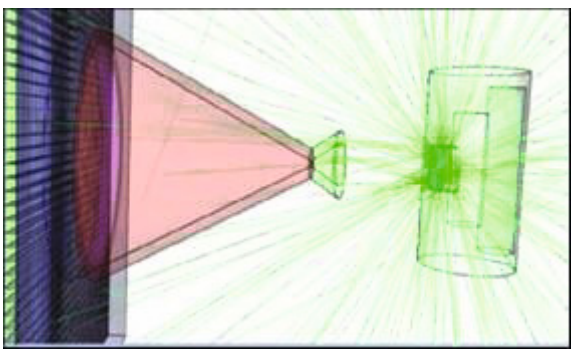

Fig. 2 Experimental model simulated by GAMOS.

From the initial file, program input data are defined. The source or generator can be associated with any type of volume designed in the geometry file and loaded with the following commands:

/Gamos/generator/addIsotopeSource SOURCE_NAME ISOTOPE_NAME ACTIVITY
/Gamos/generator/positionDist SOURCE_NAME GmGener DistPositionInG4Volumes LV_NAME

GAMOS allows to select one predefined sensitive detectors, where the events are stored if they interact within the

selected matrix and deposit an amount of energy within the energy window (20%). In this case the event is identified as a hit and it is reconstructed according to the distance between the closer interactions. This is possible by assigning this command to the crystal or pixel detector:

/gamos/assocSD2LogVol SD_CLASS SD_TYPE LOGVOL_ NAME

In this case, SD_CLASS defines sensitive detector type that is associated to the crystal and SD_TYPE allows assigning basic detector parameters: dead time, measurement time and energy resolution. The main command for classifying events detected as SPECT is the following:

/gamos/userActionSPECTEventClassifierUA

This command contains a set of programming lines where the reconstructed hit is evaluated by the deposited energy, followed by the track from the source to the detector and it is classified as SPECT or not SPECT.

For output file visualization, specific software "PUNTOS_SPECT_2010 Viewer" was used. It was developed as a result of CEADEN-CIEMAT collaboration through ITACA project. It allows to obtain the matrix dot coordinates from the processed data in a text file.

B. Validation of MC simulation

To test the accuracy of the Monte Carlo model, a neck phantom was prepared with different materials representing organ structures: neck, thyroid, trachea, and spine (Figure 1). 100μCi activity of 131I were injected inside glass vials used to represent the thyroid lobes. Two studies were carried out: first one with the phantom filled with air and the second with the phantom filled with water. Planar acquisition was made using 256*256, 200 000 Counts, window 20% (figure 3a). The images were acquired at a distance between pinhole and thyroid phantom of 6 cm. Using image processing software of the camera "JetStream" were drawn the regions of interest (ROIs) around the phantom image and the total counts of the region was determined for each image.

The same phantom was modeled; total counts values were obtained by simulating a total of 3000 million of events, which correspond to 27 minutes (1620 sec) real time for a 100μCi activity source. ROIs were positioned considering pinhole magnification. To visualized the file generated by GAMOS was used the lm2pd applications (list-mode-to-projection-data) capable to generated planar or SPECT images. The result images were processed using AMIDE software (Amide's a Medical Imaging Data Examiner) in order to obtain the total count of ROIs.

To validate the MC modeling the relationship between count rates per activity (cps/μCi) simulated and measured using a thyroid phantom were compared in the two geometries.

C. Evaluation of scatter

Once the validation process was finished, to investigate scatter, simulations were performed with different tissue thickness between the thyroid and collimator (5-15mm). The tissue density used was 0,967 g/cm3 recommended by ICRU-44. The percent of scatter of total counts in the 20% window was calculated per image.

D. Evaluation of scatter correction methods

Three of the most commonly used methods for correcting scatter have been studied through MC simulation. To evaluate their effectiveness in the clinical practice, the fraction of scattered photons was calculated for each configuration using main energy windows of 15% and 20%, centered in the 364keV photopeak. The methods used were the following [18, 19].:

· Triple energy window method (TEW) with adjacent windows of 2.5%;

· Double energy window (DW) using a k=0.5 and the

· Reduced double energy window (RDW) with an adjacent window of 2.5%.

The simulation included 4 tissue thickness between the thyroid and collimator (6, 8, 10 and 12mm). The results were compared with the scatter fraction given by the simulation, the discrepancies were evaluated and analyzed to select the best approach for the real clinical condition and geometry.

III. Results and Discussions

A. Validation of MC simulations with neck thyroid phantom.

Figure 3a shows the images obtained in the air and water experimental study with JetStream image processing software and figure 3b the GAMOS simulations results visualized with AMIDE. The regions of interest were drawn to calculate the total counts for selected ROI.

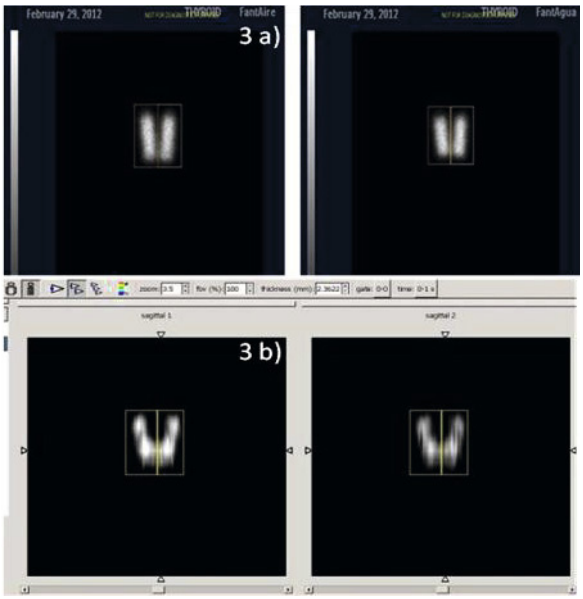

Fig. 3a) Experimental measure results visualization using JetStream. 3b) Simulated visualization results in AMIDE context. Left image obtained with the phantom full of air and to the right with the phantom full of water.

To validate the MC modeling the relationship between count rates per activity (cps/μCi) simulated and measured using a thyroid phantom were compared in the two geometries (table 1). The accuracy of the modeled geometry was verified by the good agreement between measured and simulated counts/seg in the energy window and the maximum discrepancies of 2% in the counts/sec/MBq. Those differences are not significant (p>95%). This supports the use of the programmed code for evaluating scatter and penetration of thyroids studies with pinhole.

Table 1. Experimental and simulated total counts and CPS/ μCi in air and water

Phatom´s measured results		**Phantoms modeled values**	
a) ROIs total counts			
Air	Water	Air	Water
70 062	66 526	97583	74 585
Acquisition´s Time (seg)			
1143.6	1469.4	1620*	1620*
b) Counts per second/ activity (cps/μCi)			
2.46	1.79	2.41	1.82

*estimated by the activity source´s emission.

Others authors sum to the validation process the measurement of energy spectra, but in that case it was not possible, because the standard clinic software does not allow saving the energy spectra, or the generation of energy spectra corresponding to specific regions of the image (because no energy information is saved with the position information for each event) [8, 16, 20]. However, obtained results clearly show high equivalence and demonstrate GAMOS viability to reproduce experimental data.

B. Scatter evaluation simulation's results

Using a simulated window of 20%, the medium attenuation coefficient and the scatter fraction of total counts were evaluated increasing the tissue thickness between the thyroid and collimator from 5-15mm. The scatter contribution to image was significant in the 5mm pinhole, being between 27-40% (Figure 4).

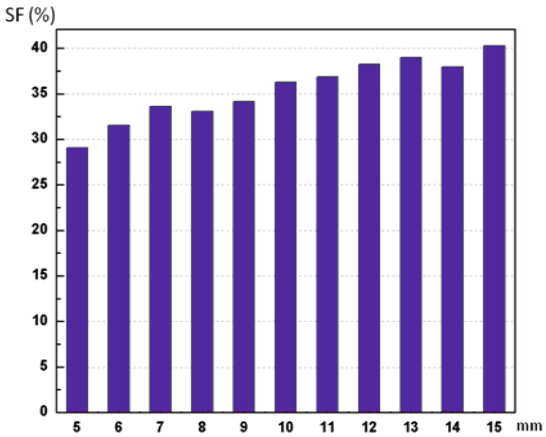

Fig. 4 Total scatter fraction vs. thickness.

Deloir at al. confirmed that in pinhole collimators the magnitudes of penetration and collimator scatter depend strongly on the collimator's size, and it could be between 40-75% (in 1, 2, 4, 8mm holes, using uniform cylinder 4,5*3cm and hotspot phantoms) [8]. The fractional contribution of penetration increases as the pinhole diameter decreases, in this case the scatter fraction was lower but significant, and the difference could be justify on the spatial distribution of the radioactive source in thyroid and the design of this particular device [5,11].

C. Evaluation of Scatter correction methods

The results of the three multi-window energy methods show significant discrepancies between them (p>95%). The discrepancies range was 9-86% (Figure 5). The behavior of the double window methods and the TEW shows significant differences, the firsts increase their discrepancies when the tissue thickness rise, meanwhile TEW decrease the discrepancies. The same situation could be observed analyz-

ing the central window size; the TEW shows better result with 20%, whereas double window methods improve their results with 15% window central size.

Fig. 5 % Discrepancies between Scatter Correction Methods and simulated total scatter vs. tissue's thickness

In general, TEW method over-estimated the scatter fraction, meanwhile double window methods under-estimated same phenomenon. However the more accuracy method was RDW 15%, which shows discrepancies between 9-16%, much less than TEW.

Many authors agreed TEW is the best method to ^{131}I image scatter correction, but always using parallel hole collimators. Scatter in ^{131}I consists of 364keV photons and high-energy photons (637 and 723 keV) *that scatter in the patient or collimator– detector system* and are detected in the 364keV photopeak window [5, 21-22]. The pinhole collimator design changes the distribution of scatter component which is completing different and especially important due to the higher probability of collimator scatter and septal penetration of HEHR or HEGP, and this could be the cause of the over-estimation.

Further evaluation of the multiple energy windows correction methods, including effects of window width and window location, needs to be performed. More work is needed to check these results, but it is desirable to have better compensation for this physical effect in clinical routine applications.

IV. CONCLUSSIONS

Sensitivity values obtained by GAMOS simulation show a good enough agreement with the experimental measurements made in Gamma Camera using a thyroid phantom. Relative deviation for water results was 1.82% and for the air 1.71%.

Similarities between the achieved results allow validating GAMOS framework applications in planar image technique and demonstrate its possibility to reproduce experimental data. Therefore the succeeded results of this comparative study allocate the further use of the GAMOS simulation platform in the adjustment of different factors that may degraded the image quantification in Gamma Cameras studies.

On the basis of the separated scatter from direct count included in window energy spectra, a preliminary evaluation of compensation method was performed. For the simulated thyroid geometry with pinhole, which is of interest in treatment planning, the RDW with 15% centered in 364keV photopeak window method provides a reasonable correction for scatter. However, the similarity between the 364keV primary and penetration energy spectra makes it difficult to compensate for these penetration events using techniques that are based on spectral analysis.

Conflict of Interest

"The authors declare that they have no conflict of interest".

References

1. Stokkel MP, Handkiewic D, Lassmann M, Dietlein M and LusterM. EANM procedure guidelines for therapy of benign thyroid disease. Eur J Nucl Med Mol Imaging 2010; 37:2218–2228.
2. Cumali Aktolun • Stanley J. Goldsmith Editors. Nuclear Medicine Therapy Principles and Clinical Applications Springer Science+Business Media New York 2013. ISBN 978-1-4614-4021-5 (eBook).
3. Liu CJ, Dong YY, Wang YW, Wang KH, Zeng QY. Efficiency analysis of using tailored individual doses of radioiodine and fine tuning using a low-dose antithyroid drugs in the treatment of Graves' disease. Nucl Med Commun. 2011; 32:227–32.
4. Merrill S, Horowitz J, Traino AC, Chipkin SR, Hollot CV, Chait Y. Accuracy and optimal timing of activity measurements in estimating the absorbed dose of radioiodine in the treatment of Graves' disease. Phys Med Biol. 2011;56:557–71.
5. Yuni K. Dewaraja, Michael Ljungberg, Alan J. Green, Pat B. Zanzonico and Eric C. Frey. MIRD Pamphlet No. 24: Guidelines for Quantitative 131I SPECT in Dosimetry Applications. J Nucl Med 2013; 54:2182–2188. DOI: 10.2967/jnumed.113.122390.
6. Willegaignon J, Guimaraes MI, Stabin MG, Sapienza MT, Michael G. Stabin, Malvestiti LF, Marília Marone, and Sordi GMAA. Corrections factors for more accurate estimates of exposure rates near of radioactive patients: experimentals, points and lines sources. Helath Phys 2007;43(6): 678-688.
7. Kobe C. et al. Radioiodine Therapy of benign thyroid disorders: what are the effective thyroidal half-life and uptake of I-131? Nucl Med Commun 2010;31:201–5.
8. Deloar H.M., Watabe H., Aoi T., Iida H. Evaluation of penetration and scattering components in conventional pinhole SPECT: phantom studies using Monte Carlo simulation. Phys. Med.Biol. 48(2003) 995–1008 (http://iopscience.iop.org/0031-9155/48/8/303)

9. Allison J et al., Geant4 developments and applications. IEEE Transactions on Nuclear Science 53: 270 -278, 2006.
10. AMIDE.exe 0.9.2 http://amide.sourceforge.net Reviewed on May 2013.
11. Rodríguez, A. Díaz, A. López, A. Palau, JM. Martín. Sensitivity comparative study in Philips Forte Gamma Camera. Proceedings of XIV Workshop on Nuclear Physics and VIII International Symposium on Nuclear & Related Techniques, WONP-NURT´2013. February, 2013, La Habana, Cuba. ISBN: 978-959-7136-98-9.
12. GAMOS 2011 User's Guide http://fismed.ciemat.es/GAMOS/GAMOS_doc/GAMOS.3.0.0/Gamos UsersGuide_V3.0.0.pdf. Reviewed on January 2013.
13. Smith M.F., Gillan D.R., Colleman E. and Jaszczak J. Quantitative imaging of I-131 Distributions in brain tumour with pinhole SPECT: a phantom study. J Nucl Med 1998; 39: 856-864.
14. Smith M F and Jaszczak R J The effect of gamma ray penetration on angle-dependent sensitivity for pinhole collimation in nuclear medicine Med.Phys. 1997; 24 (1): 701–9
15. Smith M F and Jaszczak R J. An analytic model of pinhole aperture penetration for 3D pinhole SPECT image reconstruction Phys.Med.Biol. 1998;43:761–75
16. Smith M F, Jaszczak R J, Wang H and Li J. Lead and tungsten pinhole inserts for I-131 SPECT tumor imaging: experimental and photon transport simulations IEEETrans.Nucl.Sci. 1997; 4: 474–82
17. Wanet P M, Sand A and Abramovici J. Physical and clinical evaluation of high-resolution thyroid pinhole tomography J.Nucl.Med. 1996; 37 :2017–20.
18. Kristina Norrgren Ph.D., Sigrid Leide Svegborn Ph.D., Johan Areberg Ph.D., Accuracy of the Quantification of Organ Activity from Planar Gamma Camera Images. CANCER BIOTHERAPY & RADIOPHARMACEUTICALS 2003*:* 1(18) 125-131 .
19. Habib Zaidi et al. Quantitative Analysis in Nuclear Medicine Imaging. Springer 2006. ISBN-10: 0-387-23854-9 e-ISBN 0-387-25444-7 ISBN-13: 978-0387-23854-8.
20. Ljungberg M. and Strand S. Scatter and attenuation corrections in SPECT using density maps and Monte Carlo simulated scatter functions. J Nucl Med 1990;31: 1560-1567.
21. Chiesa C, Castellani MR, Vellani C, et al. Individualized dosimetry in the management of metastatic differentiated thyroid cancer. Q J Nucl Med Mol Imaging 2009, 53:546-61
22. He B, Frey EC. The impact of 3D volume of interest definition on accuracy and precision of activity estimation in quantitative SPECT and planar processing methods. Phys Med Biol. 2010;55:3535–3544
23. Malik Mumtaz, Lim Shueh Lin, Khaw Chong Hui, Amir Sharifuddin Mohd Khir**.** SPECIAL COMMUNICATION - Radioiodine I-131 Graves' Disease. MJMS 2009; 16(1): 25-33.
24. Sisson J C , Freitas J, Ross McDougall L, Dauer L T,Hurley J R, Brierley J D , Edinboro C H et al. Radiation Safety in the Treatment of Patients with Thyroid Diseases by Radioiodine ^{131}I: Practice Recommendations of the American Thyroid Association. THYROID Volume 21, Number 4, 2011 (335-346) Mary Ann Liebert, Inc. DOI: 10.1089/thy.2010.0403
25. Sisson JC , Avram A M , Rubello D and. Gross M D. Radioiodine treatment of hyperthyroidism: fixed or calculated doses; intelligent design or science?. Eur J Nucl Med Mol Imaging (2007) 34:1129–1130.

Author: Adlin López Díaz
Institute: Hospital "Hermanos Ameijeiras"
Street: San Lázaro No 701
City: La Habana
Country: Cuba
Email: adlin2607@yahoo.es